ACCURACY OF LOCATING CIRCULAR FEATURES USING MACHINE VISION

Cheryl Sklair, William Hoff, and Lance Gatrell
Martin Marietta Astronautics Group
Denver, CO 80201

From Proceedings of SPIE Conference on
Intelligent Robotic Systems -
Cooperative Intelligent Robotics in Space II
11-15 November, 1991
Boston, Massachusetts

Accuracy of Locating Circular Features Using Machine Vision

Cheryl Sklair, William Hoff, and Lance Gatrell
Martin Marietta Astronautics Group
Denver, CO 80201

ABSTRACT

The ability to automatically locate objects using vision is a key technology for flexible, intelligent robotic operations. The vision task is facilitated by placing optical targets or markings in advance on the objects to be located. A number of researchers have advocated the use of circular target features as the features that can be most accurately located. This paper describes extensive analysis on circle centroid accuracy using both simulations and laboratory measurements. The work was part of an effort to design a Video Positioning Sensor for NASA's Flight Telerobotic Servicer that would meet accuracy requirements. We have analyzed the main contributors to centroid error and have classified them into the following: (1) spatial quantization errors, (2) errors due to signal noise and random timing errors, (3) surface tilt errors, and (4) errors in modeling camera geometry. It is possible to compensate for the errors in (3) given an estimate of the tilt angle, and the errors from (4) by calibrating the intrinsic camera attributes. The errors in (1) and (2) cannot be compensated for, but they can be measured and their effects reduced somewhat. To characterize these error sources, we measured centroid repeatability under various conditions, including synchronization method, signal-to-noise ratio, and frequency attenuation. Although these results are specific to our video system and equipment, they provide a reference point that should be a characteristic of typical CCD cameras and digitization equipment.

1. INTRODUCTION

The ability to automatically and accurately locate objects with machine vision is a key technology for robotic systems. The task can be facilitated by placing optical targets or markings in advance on the objects to be located. A number of researchers have advocated the use of circular target features, and have shown that the extracted centroids of circular features are more accurate than other common shapes, such as squares or diamonds[1,2]. The accuracy to which the centroid of a circular target feature can be located in the image plane is affected by many factors. In order to understand how accurately the feature is located, or to design a feature to meet stringent location requirements, it is essential that all known factors be investigated and their effects measured. This paper describes the accuracy analyses performed in an effort to design a Video Positioning Sensor for NASA's Flight Telerobotic Servicer (FTS).

The purpose of the Video Positioning Sensor (VPS) was to test the on-orbit fine positioning ability of the FTS manipulator, which was a space robot to assist in the assembly and servicing of the NASA space station. The robot was to be teleoperated from the Space Shuttle, with autonomous functionality added over time. To be able to adequately perform tasks in space, the manipulator had performance requirements of ±1.0", ±3.0 degrees for accuracy; 0.001", 0.01 degrees for incremental motion; and ±0.005", ±0.05 degrees for repeatability. The VPS was designed to verify manipulator accuracy, and supplement the verification of repeatability and incremental motion on the first demonstration test flight in the Space Shuttle's cargo bay. To verify accuracy, the VPS would use the wrist mounted camera to record onto the aft flight deck VCR, the views of a planar target containing 36 circular features as the manipulator toolplate moved through a sequence of positions. After the flight, the video tape would be played back, and pose of the target with respect to the camera at each of the positions would be computed and used to determine the actual locations of the toolplate in the manipulator base coordinate system. These actual positions would be compared with the commanded positions.

Tests involving the VPS were planned in three stages:

Stage 1) Ground tests, calibration and analysis.
Calibration of software camera and target models, computation of camera to toolplate and target to manipulator base transformations, and measurement of the manipulator actuator/control loop performance.

Stage 2) On-orbit tests and data collection.
Autonomous positioning of the manipulator toolplate through its sequence of tests, with the mounted targets in the wrist camera's field-of-view and video of the targets recorded at each position on the Shuttle's recording system.

Stage 3) Post-flight data analysis and report.
Analysis of the video data to determine manipulator accuracy, and provide backup analysis for repeatability and incremental motion.

Clearly, the certainty with which the manipulator fine-positioning tests could be performed depended on how accurately the VPS could determine true position of the toolplate in the manipulator base coordinate system. The primary sources of uncertainty identified in the VPS system are shown in Figure 1. They are:

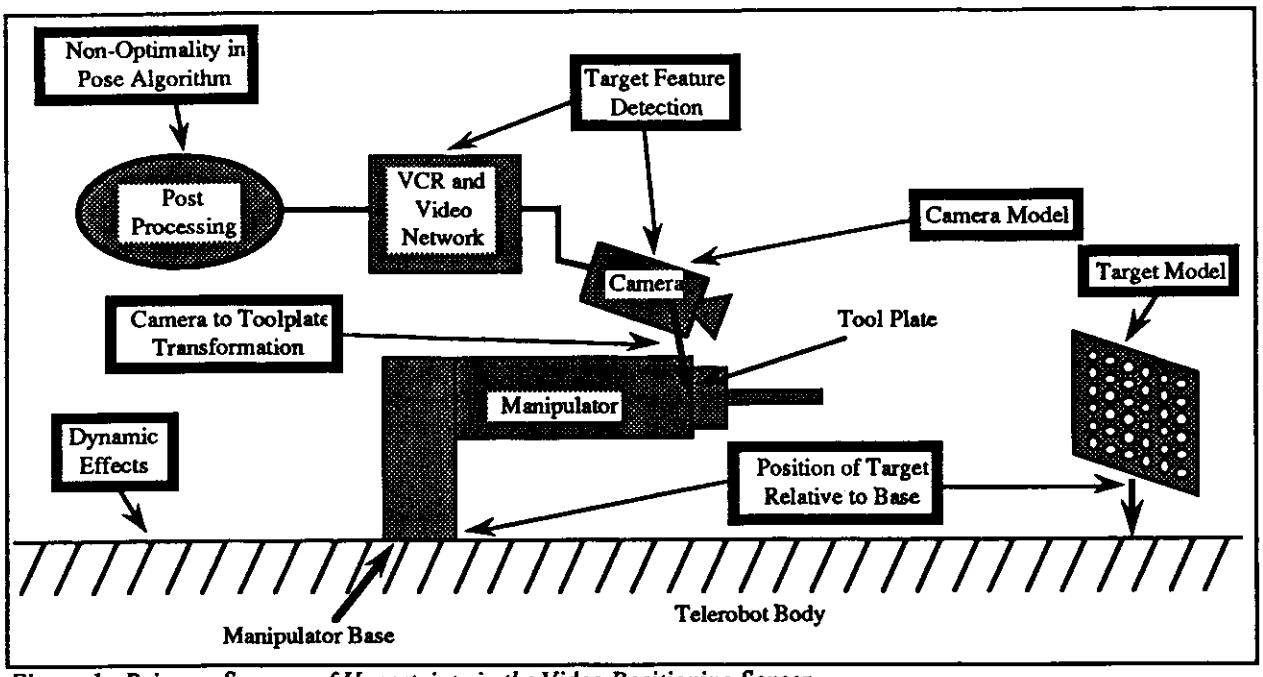

Figure 1. Primary Sources of Uncertainty in the Video Positioning Sensor.

1) Non-optimality in the pose algorithm.
   This may depend on the number of target features used, whether the target is planar or non-planar, and possibly how the algorithm computes the pose - directly or iteratively. (an iterative method may be less sensitive to inaccuracies in feature locations[3]).
2) The target model.
   How accurately the computer model of the target matches the actual target.
3) Modeling the camera sensor.
   The accuracy with which the intrinsic sensor parameters such as focal length, lens distortion, etc. have been calibrated.
4) Target feature detection.
   The accuracy with which the target features are located in the 2D image.
5) Camera to toolplate transformation.
   The accuracy in calculating the transformation from the origin of the camera to the origin of the toolplate.
6) Target position relative to manipulator base.
   The accuracy in measuring, or calibrating the location of the target origin relative to the manipulator base.
7) Dynamic effects.
   The effects of Shuttle vibrations.

Experiments were performed on all of the factors above in designing the VPS. This paper will address only the tests performed on factor 4, the accuracy of target feature detection. Section 2 will describe causes of feature location inaccuracies. Section 3 shows the results of analysis on extraction errors of circular target features.

2. CAUSES OF FEATURE LOCATION INACCURACIES

A variety of artificial or naturally occurring object markings can be used as target features in pose computation. Some of the popular markings used are circles[4,5,6], lines[7,8], and intersections of lines[9,10]. The computed image location of any type of feature will contain some error. These inaccuracies can be caused by:

1) Spatial quantization noise.
   Errors caused by projecting the objects image onto the discrete digitizing grid.
2) Surface tilt errors.
   Errors in location caused by viewing a planar target at an angle such that it is not parallel to the image plane - *i.e.*, the computed centroid of the projection of a circle viewed at an angle will not correspond with the true center of the circle.
3) Camera geometry.
   Effects caused by ignoring or using inaccurate values for the optical attributes and geometry of the camera - *i.e.*, not taking into account the distance that distortion in the lens causes an image point to be translated radially from the optical center.
4) Electronic hardware effects.
   The inaccuracies of image values caused by equipment, such as digitizers, VCR's, time based correctors, etc. - *i.e.*, the small random variations in intensity, referred to as gray level noise, and the relative shift between scan

lines due to nonperfect synchronization of the digitizer and video input, often called horizontal jitter.

The effects of some of these factors can be corrected to some extent. For example, calibrating all of the intrinsic camera attributes will correct camera effects, to the extent of the calibration accuracy. Errors caused by viewing the target at an angle can also be compensated for if an estimate of the location of the target is known or can be computed[11].

The errors caused by other factors, such as spatial quantization and hardware effects, cannot be compensated for, but they can be measured and their effects reduced somewhat. For example, the random errors of gray level noise and horizontal jitter can be reduced by averaging results from a number of images. If the centroid of the feature is to be used, spatial quantization errors can be reduced by choosing a shape with a high area to perimeter ratio, such as a circle[2].

The goal in designing the target for the VPS was to use features whose extraction errors 1) would be minimal, 2) could be understood and measured, and 3) could be reduced or removed to some extent. It was felt that the centroid (first moment) of a circle, extracted from a binary thresholded image would best meet these goals. The target was designed to be constructed of lusterless black anodized aluminum with 6 rows and 6 columns of embedded light colored iridite aluminum circles, with centers accurate to within 0.006".

3. ANALYSIS OF 2D IMAGE FEATURE EXTRACTION ERRORS USING CIRCULAR FEATURES

This section will discuss the analysis performed to measure spatial quantization, and hardware effects. Extensive analysis on the uncertainty caused by viewing the circle at an angle were performed, but the discussion would be too lengthy to be included here[11]. The tests on spatial quantization error were performed via simulation in order to isolate the effects. The tests on hardware effects used centroids extracted from real images.

Each of the experiments reported herein used a subset of the following equipment:

- 2 identical Androx ICS-400 image processing boards, one hosted by a Sun 3/160 workstation, and the other hosted by a Solbourne 5/500 workstation,
- Panasonic WVCD-20, and Pulnix TM-840 black and white CCD cameras,
- Lyon-Lamb ENC-7 Encoder/Sync Generator,
- Sony VO-8600 U-Matic VCR played through a FOR-A FA-210 time based corrector,
- Oriel optical table, with rails and various precision rotation and translation stages for precision positioning.

In performing experiments, care was taken to ensure that the camera and its cables were rigidly mounted during image acquisition, and that equipment was sufficiently warmed up. Initial experiments showed that even a slight pull of the camera cables could cause the camera to sag, and thus affect the computed image centroids. Additional tests showed the horizontal component of the computed centroid location to be unstable during the first 30 minutes or so after the cameras were first turned on, and unstable during the first 25 minutes when using the VCR and TBC.

3.1. Spatial quantization noise

Errors caused by spatial quantization (*i.e.*, the effect of projecting an object's image onto the discrete digitizing grid), were analyzed by simulation, so that the errors could be isolated. The output of a single, square, digitizer pixel in the simulation was the sum of the light intensity striking the pixel. We assumed that the circle had the maximum detectable intensity (255), and that the background had an intensity below the minimum detectable intensity (0). A pixel's output was proportional to the pixel's area covered by the circle's projection. Pixels completely covered by the circle's projection had the maximum intensity; pixels not cover any part of the projection had the minimum intensity; and pixels on the perimeter of the projection had intensities that ranged from the minimum to the maximum intensity. Following the method of Pathre[1], each perimeter pixel was subdivided into 16 by 16 subpixels. The output intensity of a perimeter pixel was the sum of the subpixels whose center was within the object's projection (with a maximum of 255).

A circle with a varying radius was synthetically projected onto the simulated digitizer. The true center of the projected circle was varied from -0.5 to 0.5 pixels in X and Y, by increments of 0.05 pixels. The projection sampling was repeated as the radius of the circle was varied from 2 to 50 pixels. The standard deviation of the errors in X or Y is given in Figure 2. These results agree with to those of Bose[2].

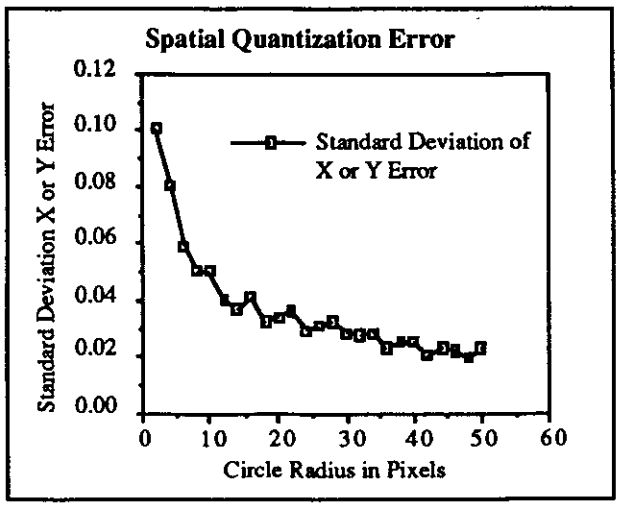

Figure 2. Standard deviation of the spatial quantization errors for X or Y.

3.2. Electronic hardware effects

The effects of electronic hardware were analyzed by measuring gray level noise, the repeatability of stationary targets through various video configurations including a simulation of the video network between the FTS wrist camera and the space Shuttle's VCR, and the effects of target size on centroid repeatability.

3.2.1. Gray level noise

Analysis of gray level noise showed it to be minimal. To perform the tests, the standard deviation of each pixel in four 30x30 regions was measured over 100 images. Each of these regions had a different, nearly constant gray level of 55, 135, 200, or 245. The average, maximum, and minimum of the standard deviations for each region are shown in Figure 3.

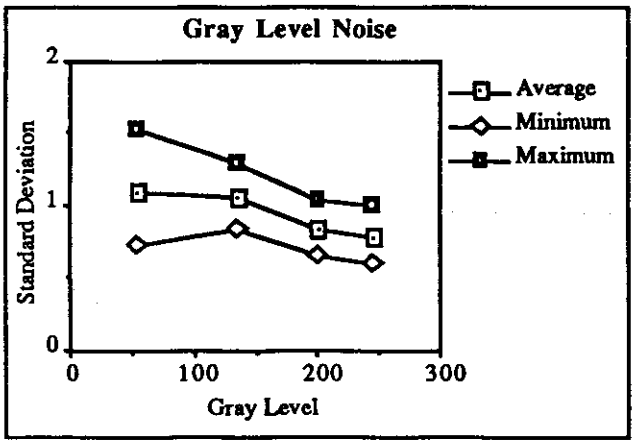

Figure 3. Standard deviations of gray levels.

The standard deviation is generally about 1.0 pixels or less, and tends to decrease as the intensity increases. In contrast, analysis on the difference between the materials used for the black background and the light colored circles showed it would be no less than 61 gray levels. Since the threshold will be set to midway between the gray levels of the black and white regions, very few pixels will be close to the threshold. Lab experiments with black paper targets on a white paper background showed very few pixels near the threshold, even with a defocused image.

3.2.2. Effects of sync and source on centroid repeatability

In TV scanning conversion, there is a one-to-one correspondence between video scan lines and frame buffer scan lines, but because of a timing mismatch there is a random relative shift between scan lines, often called horizontal jitter. This jitter was measured electronically by Lenz and Tsai[12] on several different cameras to average 0.1-0.3 pixels in an individual scan line. Since we were concerned with the effects of jitter on centroid location, our investigation approach was to measure the repeatability of the centroid location of a stationary target circle.

The goals of the experiments were to determine:

1. How much uncertainty jitter causes in a single image,
2. The extent that the uncertainty can be reduced by combining the results of multiple images,
3. How the uncertainty changes as the synchronization method and video configuration change.

The process of the experiment involved digitizing, and computing and recording the centroid of a stationary circular target over an extended period of time. The images were continuously processed at a rate of about 15 per second. The recorded data was then analyzed. The N recorded centroids were read in and groups of M centroids were averaged, giving a reduced list of N/M centroid locations. N typically ranged from 500 to 25,000 and M from 1 to 32. From this reduced list of centroids, the following statistics were computed:

- the average and standard deviations of x (horizontal component), y (vertical component), and area,
- the autocorrelation of x, y, and area,
- a test to check the randomness of x, y, and area.

This method was used for testing the camera-digitizer configurations shown in Figure 4. In Figure 4a, the simplest configuration, the video goes directly into the digitizer and the camera supplies the sync. In Figure 4b, the digitizer board originates the sync (separate horizontal and vertical) for the camera. In Figure 4c, composite sync is externally generated and supplied to both the camera and digitizer. Figure 4d shows the video recorded onto a VCR and then played back into the digitizer. This last setup was the likely scenario for the FTS. The camera would be locked up to an external sync source on the Shuttle, and record directly into a VCR. The video would then be played back into a digitizer on the ground.

3.2.2.1 Video configuration 1: camera-driven sync

A plot of the x, or horizontal location of the centroid as a function of time is shown in Figure 5a. The data is periodic with a period of approximately 5 seconds and an amplitude of about 0.03. The y centroid location and the target area, shown in Figures 5b and 5c, are also periodic, although less prominently so. These tests were performed with the Androx board hosted by the Sun workstation using the Panasonic camera.

The cause of the periodicity is not known, and it is not restricted to the particular digitizer and camera used. The same experiment was performed on the Androx board on the Solbourne host in another laboratory, using the Pulnix camera, and the results were virtually the same. We also tried using incandescent lighting instead of fluorescent lighting, with no change.

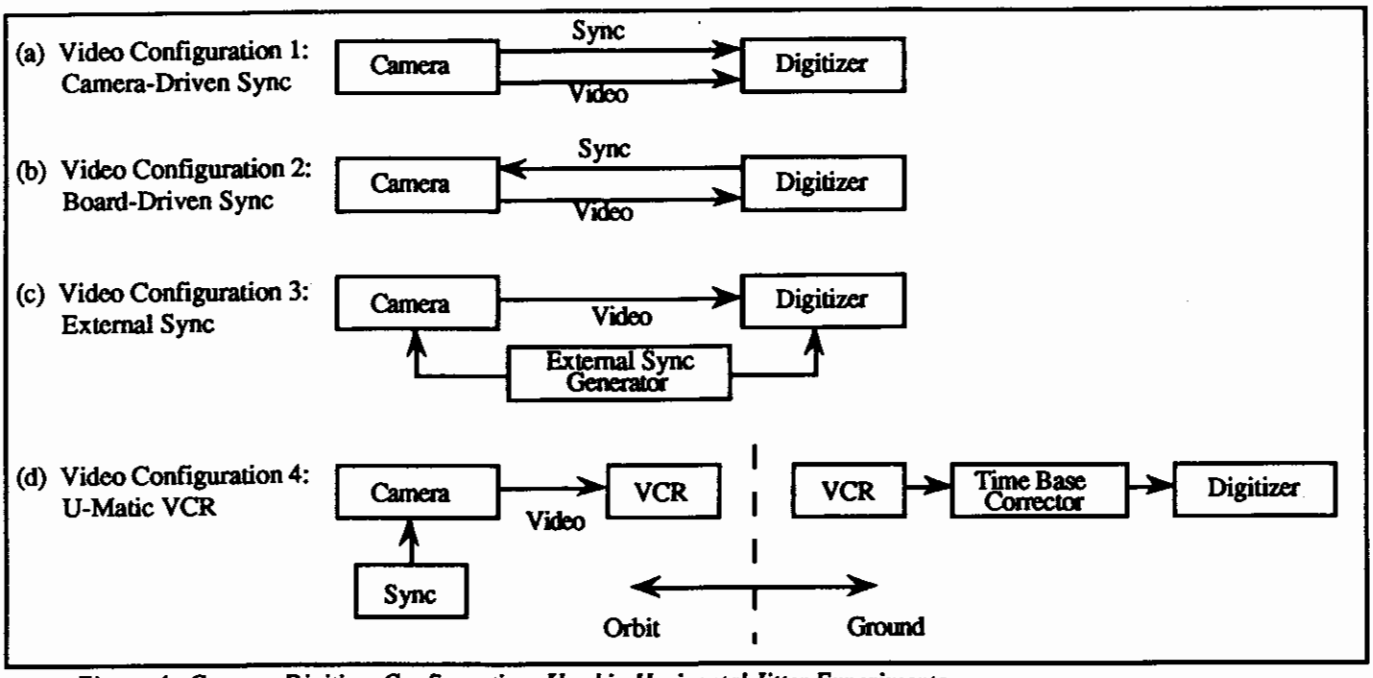

Figure 4. Camera-Digitizer Configurations Used in Horizontal Jitter Experiments

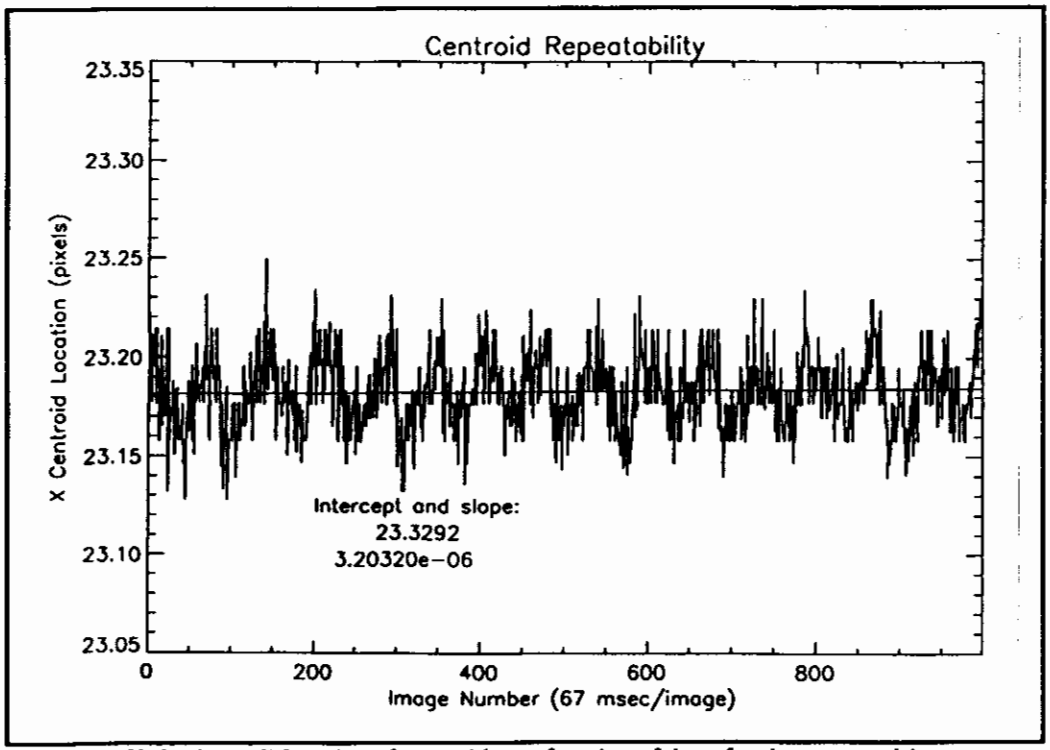

Figure 5a. X (horizontal) location of centroid as a function of time, for the camera driven sync configuration. Period is about 5 seconds. Data taken with the Panasonic WVCD20 camera.

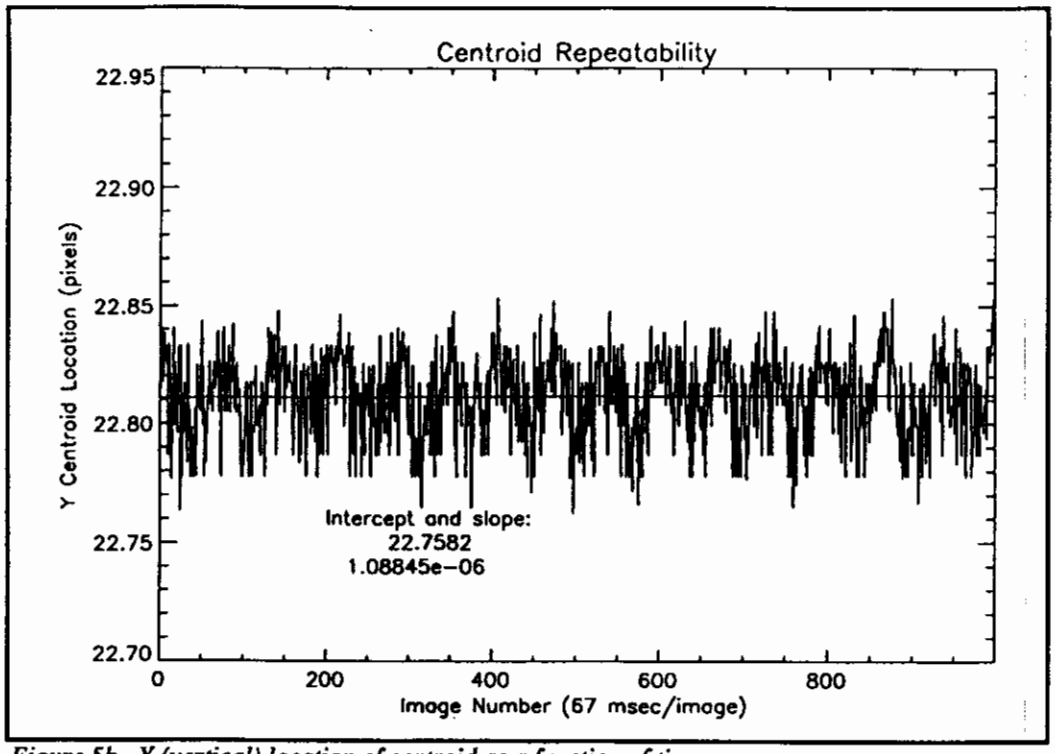

Figure 5b. Y (vertical) location of centroid as a function of time.

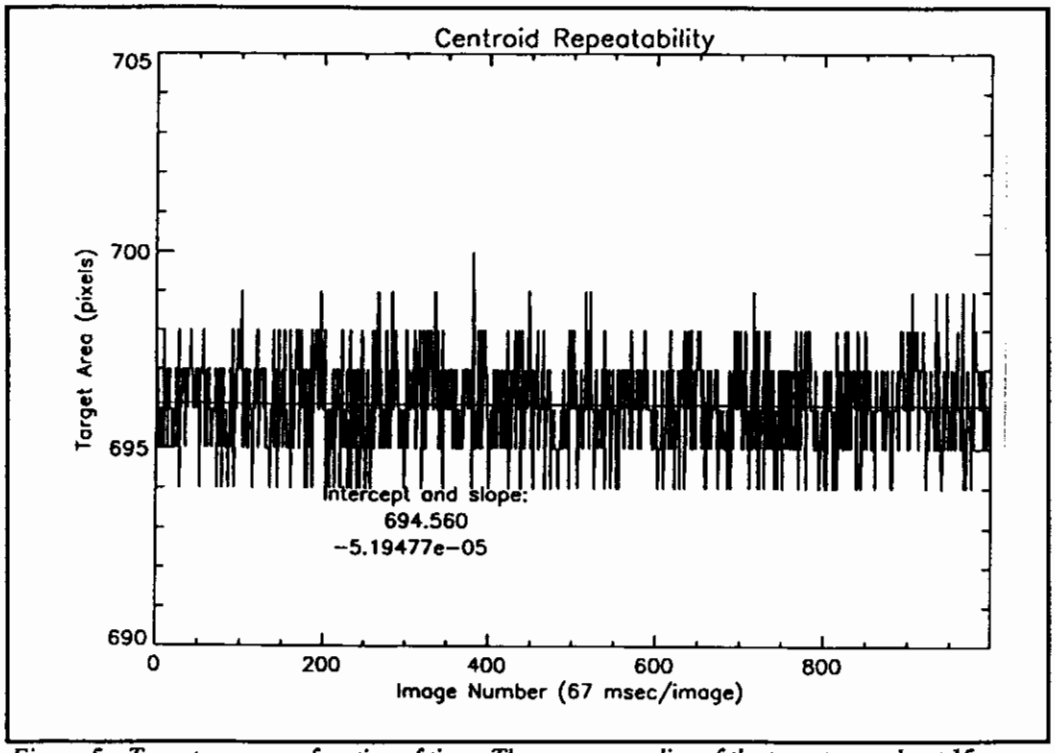

Figure 5c Target area as a function of time. The average radius of the target was about 15 pixels.

The periodicity becomes more evident when the autocorrelation function of the data is investigated. The autocorrelation value $r(u)$ for a sequence of data values $x(i)$, $i=1..N$ is defined as

$$r(u) = \frac{\sum_{i=1}^{N-M}[x(i)-\bar{x}][x(i+u)-\bar{x}]}{N\sigma_x^2}, \text{ for } u = 0..M \quad (1)$$

The autocorrelation was performed on a sequence of 10,000 images (N=10,000) using lag values from 0 to 500 (M=500). The results of the autocorrelation for the x and y components, shown in Figures 6a and 6b, reveal an almost identical periodic autocorrelation, with a period of about 75 images, or 5 seconds. The results from the area values showed a small amount of correlation at small lag values, tapering off at lag values exceeding about 150 images, or 10 seconds.

The level of significance of the autocorrelation values may be estimated by the following method[13]. When the number of pairs N-M is large, the sampling distribution of correlation coefficients for a truly random series is nearly normal and is given by

$$\sigma_r = \frac{1}{\sqrt{N-M-1}} \quad (2)$$

The level of significance for the 95% probability level for a normally distributed random variable is $r = 1.96\sigma_r$. When N-M = 9500, r at the 95% confidence level is 0.02. Thus, autocorrelation values greater than 0.02 may be considered to be significantly different from that expected for a truly random sequence. The x and y values are significantly correlated at almost all the lag values of up to 500 images, or 33 seconds.

Another test was made to see if the results varied over time. Eight separate runs were made at intervals of about 2 to 10 minutes between the runs. In each, the centroid location in 1000 images was found, and the average location and standard deviation was computed. The results showed that the averages and standard deviations were relatively constant over this short time frame. For these runs, the average standard deviations for x, y, and area were 0.0187, 0.0177, and 1.128 pixels respectively.

Finally, the effects of averaging groups of centroids locations was tested. The centroid locations from N = 10,000 consecutive images were computed and stored. The values of each group of M images were averaged to yield a reduced list of N/M centroid locations, where M varied from 1 to 32 (0.067 to 2.1 seconds). The results for x and y are given in Figures 7a, 7b. This figure combines the results from the other video configurations, also.

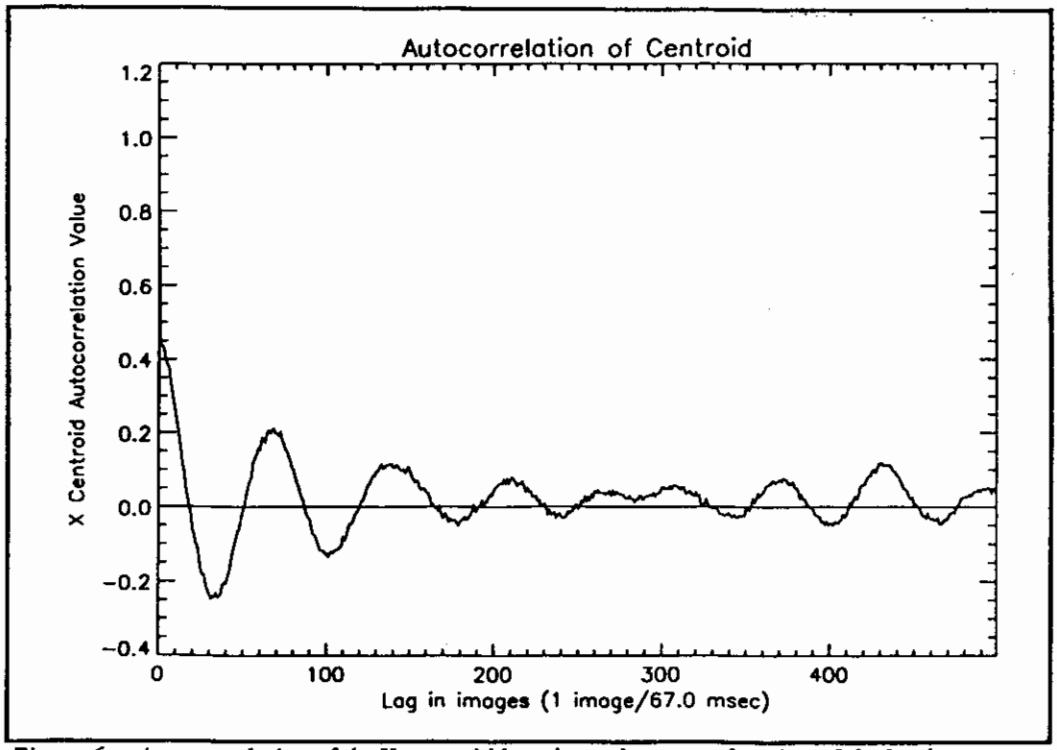

Figure 6a. Autocorrelation of the X centroid location values, as a function of the lag between images. Camera-driven sync. Data taken from a sequence of 10,000 images.

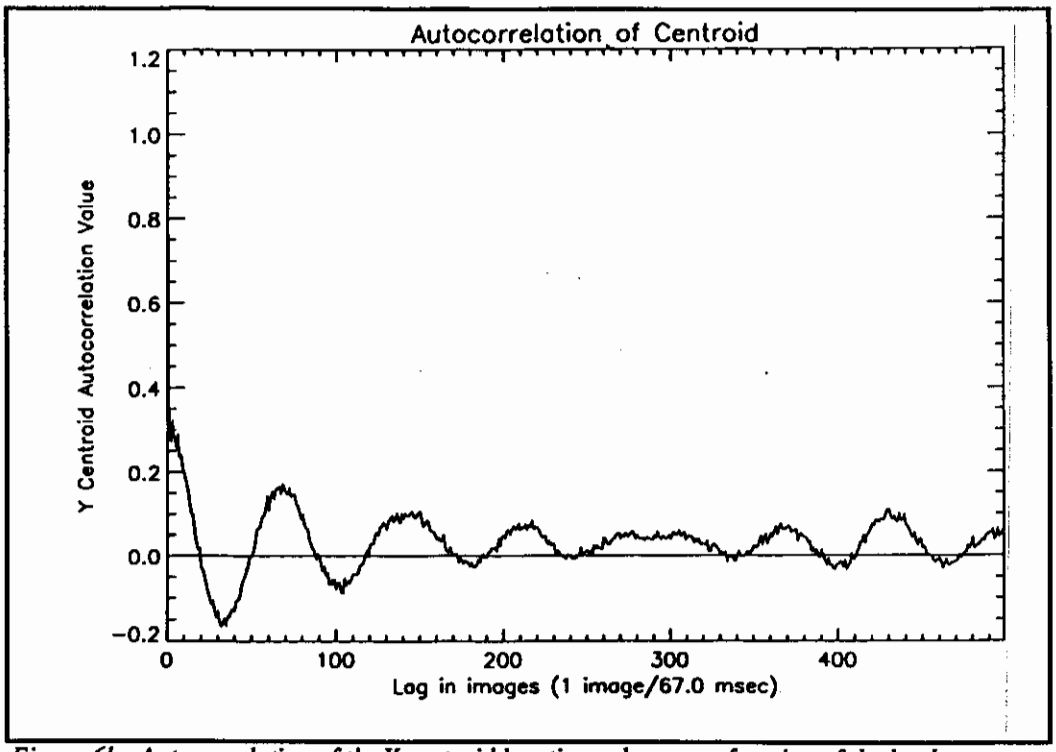

Figure 6b. Autocorrelation of the Y centroid location values, as a function of the lag between images. Camera-driven sync. Data taken from a sequence of 10,000 images.

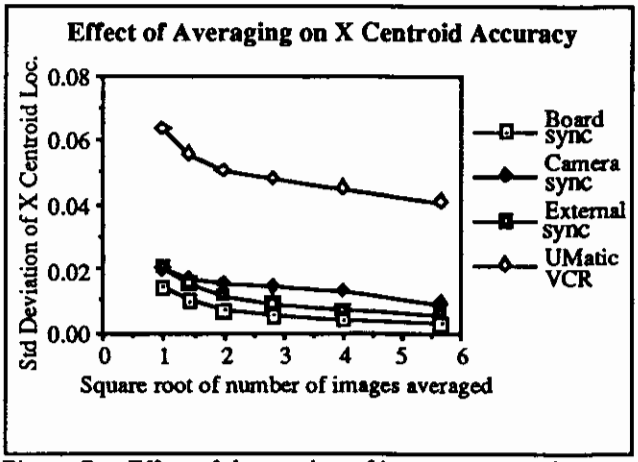

Figure 7a. Effect of the number of images averaged on the standard deviations of the x location of the centroid. For U-Matic configuration, data taken from 25,000 images, For other configurations, data taken from 10,000 images. Images taken approximately 15/second.

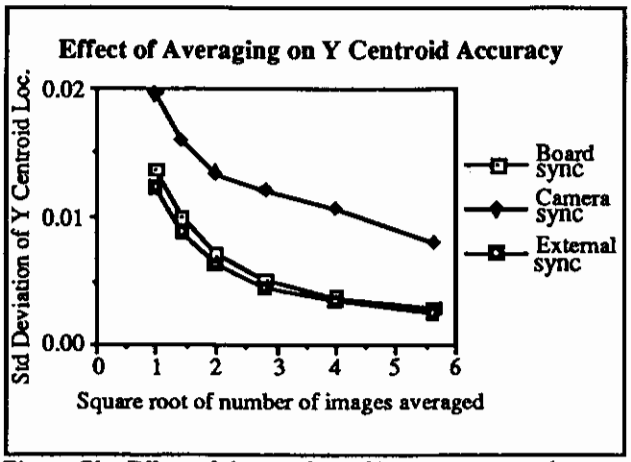

Figure 7b. Effect of the number of images averaged on the standard deviation of the y location of the centroid. U-Matic data not displayed because of spurious values in the y location data (see text)

3.2.2.2. Video configuration 2: board-driven sync

In video configuration 2, the digitizer board originates the sync for the camera. A plot of the horizontal location of the centroid as a function of time shown in Figure 8 displays no obvious periodicity in the data. Tests on autocorrelation showed the values to hover at or below the 0.02 significance value, except for lag values of 30 images or less, where they were slightly larger.

To see if the results varied over time, an interval test, as described in configuration 1 was performed. The results showed the averages and standard deviations to be relatively constant over the short time frame, with average standard deviations for x, y, and area as 0.0221, 0.0076, and 0.813 pixels respectively.

The results of tests on the effects of averaging groups of centroid locations, as described in configuration 1, are shown in Figures 7a and 7b.

3.2.2.3. Video configuration 3: external sync

In video configuration 3, an external sync source (the Lyon Lamb Enc-7) supplies composite sync to the digitizer and the camera. The horizontal location of the centroid as a function of time is shown in Figure 9. A slight periodicity is evident in the data. The autocorrelation tests showed a small periodic correlation, with a period of about 150 images, or 10 seconds.

The results of the time interval test showed the results to be stable over time. The average standard deviations for x, y, and area were 0.0202, 0.0121, and 1.078 pixels.

The results of tests on the effects of averaging groups of centroid locations, as described in configuration 1, are shown in Figures 7a, and 7b.

3.2.2.4. Video configuration 4: U-Matic VCR

In video configuration 4, an external sync source (the Lyon Lamb Enc-7) supplies composite sync to the camera, which then sends video (plus sync) to be recorded on the U-Matic VCR. The video is then played back into the digitizer.

nitial tests on the location of the centroid as a function of time showed a definite long-term trend in the data. To better observe the behavior, about 30 minutes of video was recorded onto the VCR. The video was played back and 25,000 images digitized, and their feature centroids recorded in a file. Groups of 25 consecutive centroids were then read in and averaged to produce a list of 1000 centroids. The block-averaged x locations are showed in Figure 10. A repetitive long-term fluctuation, with a period of about 400 groups (approximately 12 minutes), is clearly evident.

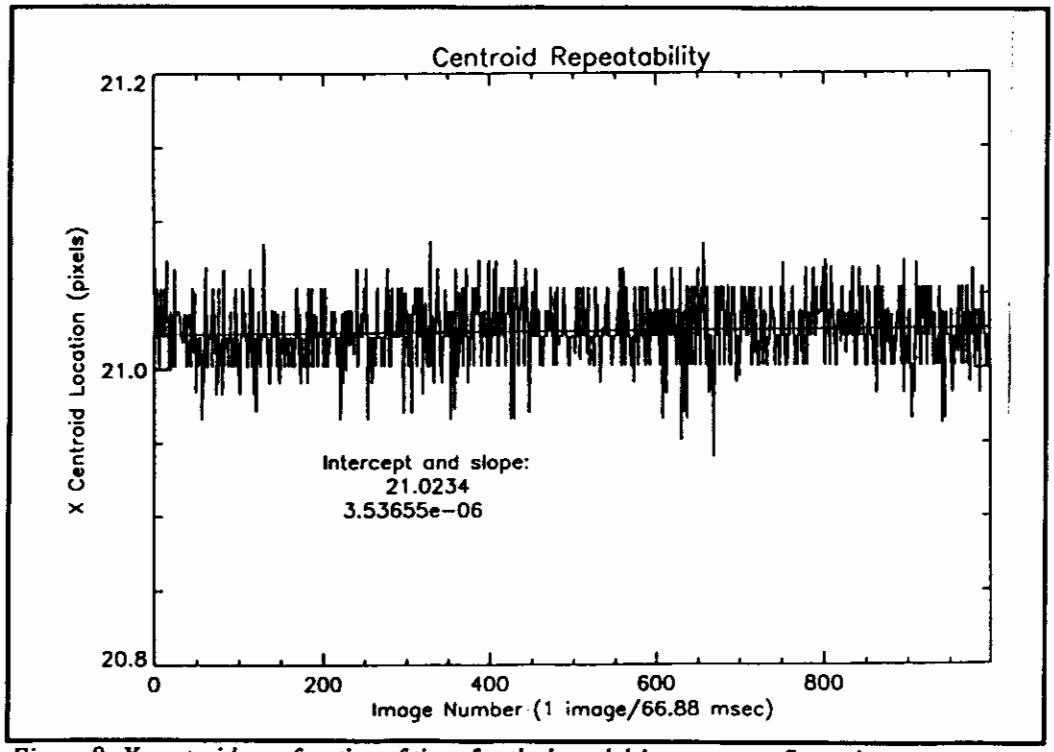

Figure 8. X centroid as a function of time, for the board driven sync configuration

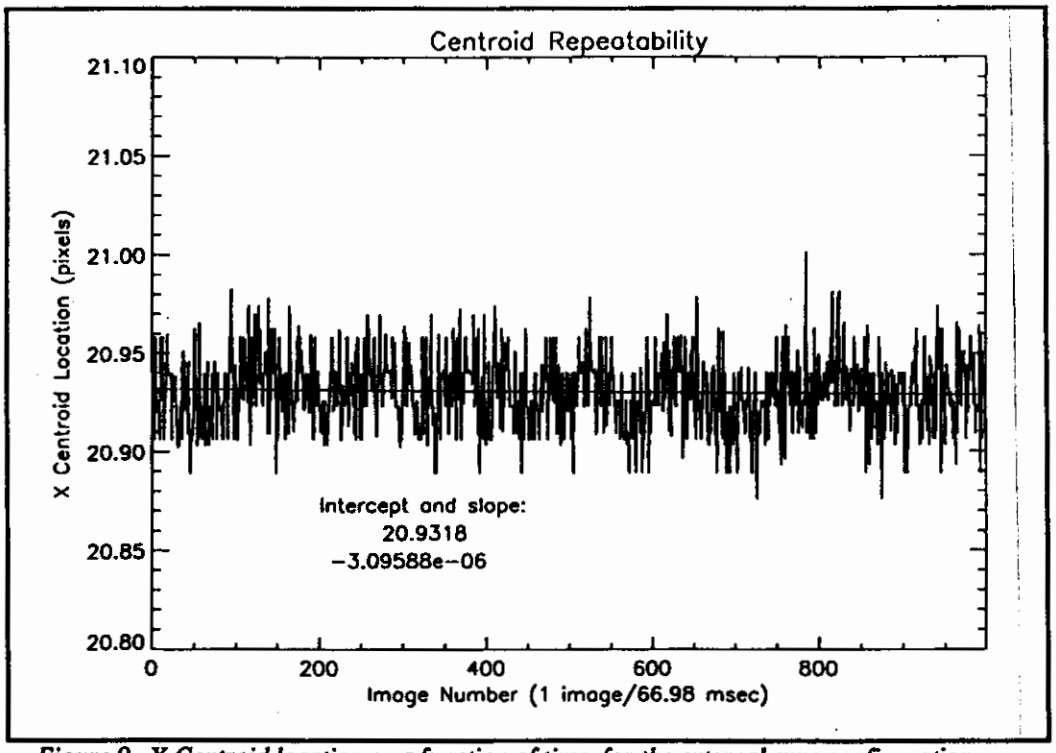

Figure 9. X Centroid location as a function of time, for the external sync configuration.

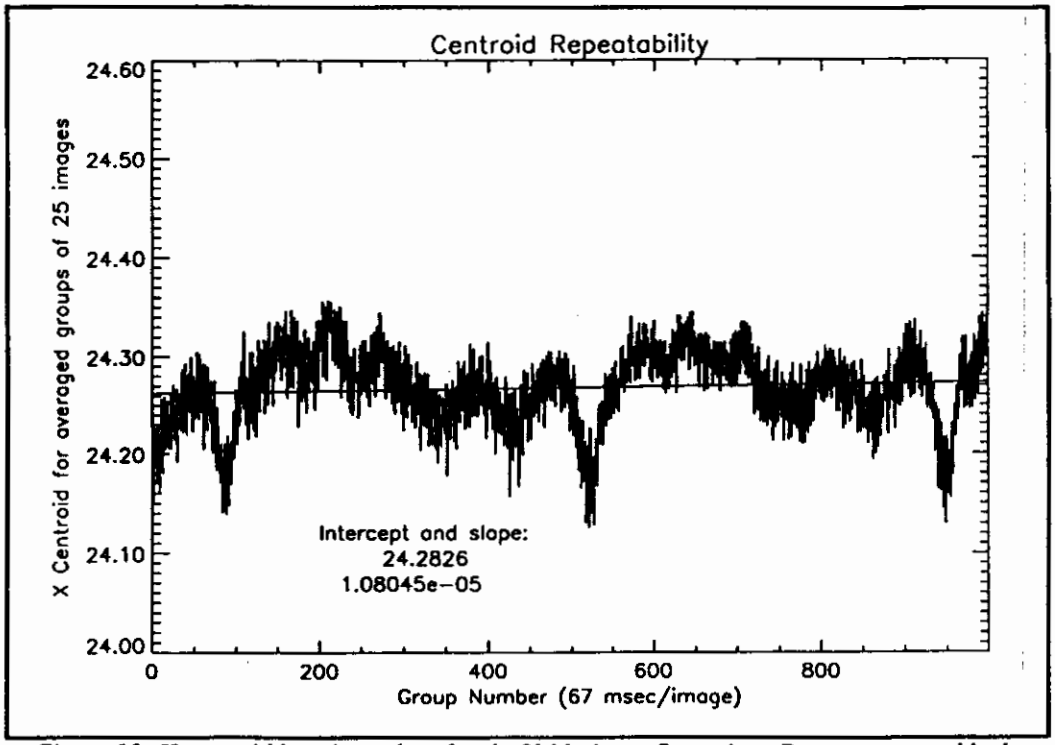

Figure 10. X centroid location values for the U-Matic configuration. Data represents block-averages from a sequence of 25,000 images.

To see if the slow shift in centroid locations was on the videotape, the video tape was played back and images digitized and centroids computed and recorded two more times. Each time, the video was started from the same frame. The block averaged x locations showed the same long-term signal, but the phase of the signal was shifted in each. Since the same video was used in each case, the shift in centroid location cannot be on the videotape.

There was no corresponding long term signal evident in the block average y locations, but there was a small interval (about 30 seconds) in each case where the y location of the centroid dropped about 1.0 pixel below its average value. The time at which this occurred was different for each case, again indicating that the cause is was not on the videotape. The only other novel thing about this configuration (besides the VCR) is the time base corrector through which the video is played. The cause of the drop is unknown, but it is easy to notice when it occurs, as long as data is taken for longer than 30 seconds.

Autocorrelation tests on x locations for lag values of 0 to 500 showed significant autocorrelation for all lag values, as would be expected from the slow fluctuations in the average x location.

As in previous sections, tests on the effect of averaging locations were made. For this test though, the centroid locations from N=25,000 images were used. The results are shown in Figures 7a .

In conclusion, the standard deviation of the error in the x, or horizontal location of the centroid due to horizontal jitter ranges from about 0.02 (for the board-driven sync) to 0.06 pixels (for the U-Matic configuration). The U-Matic VCR configuration was much worse than the other configurations, and we do not know the reason for the long-term fluctuation in the data. The errors for all of the configurations can be reduced by about 30% or more by averaging the centroids from 32 images. The error in the y location is less than the error in the x location.

3.2.3. Effects of video link on centroid repeatability

The effects of the video link on centroid repeatability were experimentally measured. Although our experiments focused on the characteristics of the Flight Telerobotic Servicer video system, the results were so conclusive that they should apply to a wide range of video systems. We designed a system of circuitry and cabling to simulate the video link from the FTS wrist camera to the Space Shuttle's VCR. We specifically looked at three effects: (1) video link electronic noise, (2) video signal amplitude, and (3) signal distortion due to frequency attenuation. Video link noise was of concern because it was thought that the robot's actuators could have introduced some electronic noise into the video cable, since the cable (a flat conducting cable) passed in close proximity to the actuators. Video signal amplitude and frequency attenuation were of concern because the long path length of the video cable could have reduced the signal amplitude and attenuated higher frequencies.

3.2.3.1. Noise tests

We trained a black and white CCD camera on a target consisting of a set of white-on-black dots. The camera signal was 1.5 volts peak-to-peak. We first added coherent noise, consisting of a 25 KHz square wave (10% duty factor), and later non-coherent noise, which was simulated by sweeping a saw tooth wave (10% duty factor) continuously from 100 KHz to 10 MHz. In both cases, we measured centroid repeatability as a function of noise amplitude, for amplitudes ranging from 15 millivolts to 150 millivolts. The results were similar for both types of noise: the standard deviation of the centroids was highest when the noise level was 150 millivolts (about 0.05 pixel horizontally, 0.03 vertically), and decreased rapidly as the noise amplitude decreased, leveling out when the noise level was 15 millivolts (about 0.02 pixel horizontally, 0.01 vertically). We repeated the tests with the video signal generated by a VCR/Time Base Corrector combination instead of a camera, and found even less variability in the repeatability. We concluded that even a worst case abnormally high level of noise has little effect on centroid repeatability.

3.2.3.2. Signal amplitude tests

Using the same camera and target scene, we reduced the signal amplitude in intervals from 1.5 volt peak-to-peak down to about 0.6 volt peak-to-peak. There was almost no change in centroid repeatability (less than 0.004 pixels) either horizontally or vertically, as the signal amplitude varied. The same results were obtained with the VCR/Time Base Corrector input.

3.2.3.3. Frequency attenuation tests

We next tested the effect of frequency attenuation, by varying the video link length. A twisted pair cable was varied in length from zero to over 700 feet. Again, there was very little change in centroid repeatability (less than 0.007 pixels) either horizontally or vertically, as the signal amplitude varied. The same results were obtained with the VCR/Time Base Corrector input.

In conclusion, the video link had little or no effect on centroid repeatability over a wide range of reasonable parameters for noise, amplitude, and frequency attenuation. These results are understandable: Since the target dots are large, high contrast features, it is reasonable that noise should have a small effect. Also, the centroid should be unaffected by overall intensity changes or by low pass filtering. Therefore, we conclude that target circle feature extraction is robust with respect to video link effects.

3.2.4. Effects of target area on centroid repeatability

The effects of target area on centroid repeatability were analyzed using video configuration 1, camera-driven sync (Figure 4a). If the jitter of individual scan lines is truly uncorrelated to other scan lines, one would expect the uncertainty in centroid location to decrease as the area of the target increased.

Five targets ranging from 0.5" to 1.5" radii were used. These sizes corresponded to image radii of 28 to 84 pixels. Each target was placed in front of the camera near the image center, the target centroids for 1000 images were computed, and the statistics on the repeatability calculated. This test was repeated 5 times for each target. The *average* of the 5 standard deviations of the centroids for each target are shown in Figure 11. The standard deviation of the vertical values decreases only slightly, while that of the horizontal values decreases significantly, which is what would be expected of errors caused by scan line jitter. Therefore, at least for the given video configuration, increasing the size of the target should increase its location accuracy.

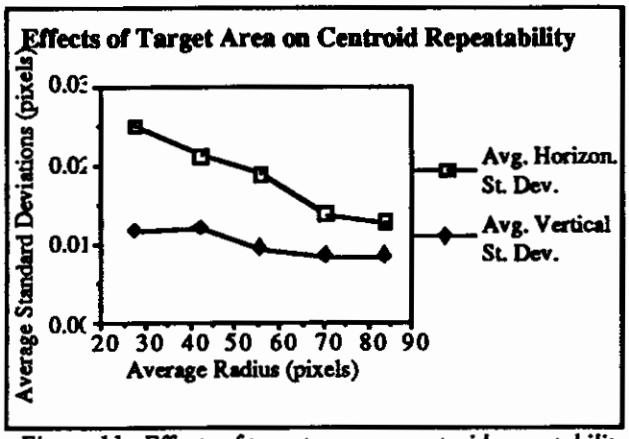

Figure 11. Effects of target area on centroid repeatability.

3.3. Testing total centroid inaccuracy

For the final experiment, we wanted to see if we could estimate total centroid inaccuracy using predicted repeatability errors and spatial quantization errors from the simulation. The test used video configuration 1, camera-driven sync, and a black planar target containing 35 white circular features. The target was mounted on a precision translation stage on the optical table in front of the camera. The centroids of 9 of the target features were computed as the target was moved small, precise steps of 0.5mm via the micrometer on the translation stage. At each step, the centroids of the 9 features were computed in 50 images, and then averaged. Figure 12 shows the locations of the features selected from the target, and Table 1 shows the average horizontal move for each point, in pixels, and the standard deviations of the move. One would expect points in the same columns (*i.e.* points 1, 4, 7) to have nearly the same average moves.

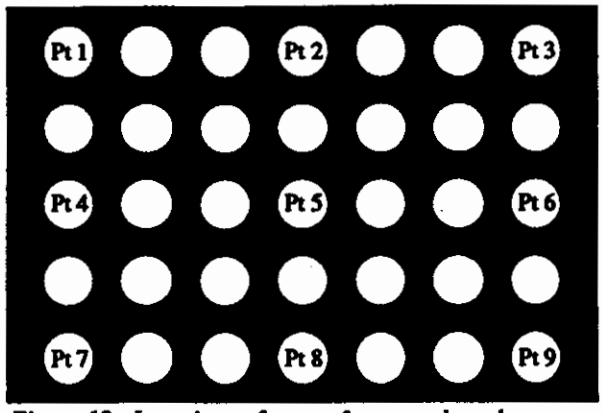

Figure 12. Locations of target feature selected.

Table 1. Average moves and standard deviations of the moves for each target feature.

Point Number	Average Horizontal Move (pixels)	Standard Deviation of Moves (pixels)
1	0.6424	0.04933
2	0.6878	0.01438
3	0.6611	0.06840
4	0.6379	0.03635
5	0.6942	0.03746
6	0.6537	0.06357
7	0.6290	0.04081
8	0.6812	0.02662
9	0.6481	0.02884

The circular features for this test had radii of approximately 20 pixels which was about the same size as the circle used in the tests in section 3.2.2.1. From these results, the standard deviation of the the repeatability of the target with 50 centroids averaged is approximately 0.01 pixels and the simulation of quantization errors from section 3.1. (Figure 2) gives a standard deviation value of 0.033835 for a circle of radius = 20. Using these values in equation (3), the total error should be 0.03528 pixels. The average of the standard deviations of points in Table 1 is 0.0406407, a difference of 0.0053607 pixels.

$$\sigma_t = \sqrt{\sigma_j^2 + \sigma_q^2} \qquad (3)$$

where:

σ_t = standard deviation of total error,

σ_j = standard deviation of the repeatability of the circle

σ_q = standard deviation of the quantization error.

4. SUMMARY

We have analyzed the main contributors to centroid error and have classified them into the following: (1) spatial quantization errors, (2) errors due to signal noise and random timing errors, (3) circle tilt errors, and (4) errors in modeling camera geometry. It is possible to compensate for some of the error caused by circle tilt and camera characteristics, but the errors caused by spatial quantization and the electronic hardware can only be measured and their effects reduced somewhat.

Our results demonstrating that spatial quantization noise can be reduced by increasing the size of the circle are similar to those of Bose[2]. We found gray level noise, and the effects of the video link between the Space Shuttle's VCR and the FTS wrist camera to be insignificant. The effects of scan line jitter varied with the video configuration, and the VCR configuration was significantly worse than the others. A long term (approx. 12 minute) trend in the horizontal location of the centroid was present in the VCR configuration, and its cause is not known. We also demonstrated how the effects of scan line jitter can be reduced by averaging the centroid results of a number of images, and by increasing the size of the circle.

5. REFERENCES

1. Pathre, U., "Three-Dimensional Object Recognition From Single Tow-Dimensional Images," Ph.D. thesis in Mechanical Engineering, Texas A&M University, December 1989.

2. Bose, C. B., and I. Amir, "Design of Fiducials for Accurate Registration Using Machine Vision", *IEEE Transaction on Pattern Analysis and Machine Intelligence*, Vol. 12. No. 12, December 1990., pp. 1196-1200.

3. Krishnan, R., H. Sommer III, and P. Spidaliere, "Monocular Pose of a Rigid Body Using Point Landmarks," *submitted to Computer Vision, Graphics, and Image Processing*, 1990.

4. Tsai, R., and R. Lenz, "Overview of a Unified Calibration Trio for Robot Eye, Eye-to-Hand, and Hand Calibration using 3D Machine Vision," *SPIE Vol. 1003, Sensor Fusion: Spatial Reasoning and Scene Interpretation*, 1988, pp. 202-213.

5. Cornils, K., and P. Goode, "Location of Planar Targets in Three Space from Monocular Images," *Goddard Conference on Space Applications of Artificial Intelligence and Robotics*, May, 1987.

6. Sklair, C., L. Gatrell, W. Hoff, and M. Magee, "Optical Target Location Using Machine Vision in Space Robotics Tasks," *SPIE Vol. 1387, Cooperative Intelligent Robotics in Space*, 1990, pp. 380-391.

7. Lowe, D., "Three-Dimensional Object Recognition From Single Two-Dimensional Images," *Artificial Intelligence*,, Vol. 31, No. 3, March 1987, pp. 355-395.

8. Y. Liu, T. Huang, and O. Faugeras, "Determination of Camera Location from 2-D to 3-D Line and Point Correspondences, *IEEE Transactions on Pattern Analysis and Machine Intelligence*, Vol. 12, No. 1, January 1990, pp. 28-37.

9. Tsai, R., "A Versatile Camera Calibration Technique for High-Accuracy 3D Machine Vision Metrology Using Off-the-Shelf TV Cameras and Lenses," *IEEE International Conference on Robotics and Automation*, April 1988, pp. 544-461.

10. Thompson, D., and J. Mundy, "Three-Dimensional Model Matching from an Unconstrained Viewpoint," *IEEE International Conference on Robotics and Automation*, March 1987, pp. 208-220.

11. Hoff, W., *et al*, "Compensating For Centroid Errors Due To Surface Tilt", *submitted to: IEEE Conference on Computer Vision & Pattern Recognition*, June 15, 1992.

12. Lenz, R., and R. Tsai, "Techniques for Calibration of the Scale Factor and Image Center for High Accuracy 3D Machine Vision Metrology," *IEEE Transaction on Pattern Analysis and Machine Intelligence*, Vol. 10, No. 5, September 1988, pp. 713-720.

13. Brooks, C., and N. Carruthers, *Handbook of Statistical Methods in Meteorology*, Her Majesty's Stationary Office, London, 1953.